J Mater Sci (2007) 42:4792–4800
DOI 10.1007/s10853-006-0830-0

Fabrication of carbon nanofiber(CNF)-dispersed Al_2O_3 composites by pulsed electric-current pressure sintering and their mechanical and electrical properties

Ken Hirota · Yuichi Takaura · Masaki Kato · Yoshinari Miyamoto

Received: 20 January 2006 / Accepted: 21 August 2006 / Published online: 19 March 2007

Abstract Dense Al_2O_3-based composites (≥99.0% of theoretical) dispersed with carbon nanofibers (CNFs) were fabricated using the pulsed electric-current pressure sintering (PECPS) for 5 min at 1300°C and 30 MPa in a vacuum. The dispersion of CNFs into the matrix depended much on the particle size of the starting Al_2O_3 powders. Mechanical properties of the composites were evaluated in relation with their microstructures; high values of three-point bending strength σ_b (~800 MPa) and fracture toughness K_{IC} (~5 MPa·m$^{1/2}$) were attained at the composition of CNF/Al_2O_3 = 5:95 vol%, which σ_b and K_{IC} values were ~25% and ~5%, respectively, higher than those of monolithic Al_2O_3. This might be due to the small Al_2O_3 grains (1.6 μm) of dense sintered compacts compared with that (4.4 μm) for the pure Al_2O_3 ceramics, resulting from the suppression of grain growth during sintering induced by uniformly dispersed CNFs in the matrix. Electrical resistivity of CNF/Al_2O_3 composites decreased rapidly from >10^{15} to ~2.1×10^{-2} Ωm (5vol%CNF addition), suggesting the machinability of Al_2O_3-based composites by electrical discharge machining.

K. Hirota (✉) · Y. Takaura · M. Kato
Department of Molecular Science and Technology, Faculty of Engineering, Doshisha University, Kyo-Tanabe, Kyoto 610-0321, Japan
e-mail: khirota@mail.doshisha.ac.jp

Y. Miyamoto
Joining and Welding Research Institute, Osaka University, Ibaraki, Osaka 567-0047, Japan

Introduction

Since the revival of carbon whiskers as carbon nanotubes (CNTs) which have been reported first by Iijima in 1991 [1], and carbon nanofibers (CNFs) for composite applications, there has been increasing research and development into methods of dispersing and functionalizing these materials to exploit their theoretical potential as superior functional additives and reinforcements. Although academic researches and scientific interests have been mainly focused on single-wall nanotubes (SWCNT) and multi-wall nanotubes (MWCNT), many of the world technical achievements can directly be transformed on carbon nanofibers (CNFs) [2]. At least in the composite application areas CNFs are considered as relatively thick and long nanotubes without compromising on composite properties in comparison with CNTs (SWNT and MWNT) dispersed in composites, especially with respect to realistic time to market scenarios [3].

Thus, carbon nanofibers (CNFs) have lately attracted remarkable attention as reinforcements of materials because of their exceptional mechanical (the tensile strength of ~2.20 GPa and modulus of 100–300 GPa for a 0.15 μm diameter nanofibers) and electrical properties (graphitized CNFs exhibits a high conductivity of (1×10^6 Sm^{-1}) [2]. However, studies on the ceramic-CNF composites have been rarely reported. One of the reasons of this, the mechanical properties of these composites have not been so much improved with addition of CNTs (CNFs); this has been explained by lack of good dispersion of CNTs (CNFs) and the poor cohesion between the CNTs (CNFs) and the matrix. Therefore, the fabrication of homogeneous nanocomposites with carbon nanotubes (CNTs) and also carbon nanofibers (CNFs) remains a technical challenge.

In the present study, fabrication of alumina-CNF composites has been tried to investigate the effect of CNFs addition on the mechanical and electrical properties. Previous studies [4–6] made it cleared that when CNTs were added to an alumina and sintered by the hot press and/or hot extrusion method, the mechanical strength of the composites was not improved; this was attributed to aggregation (or inhomogeneous dispersion) of CNTs in the composite materials because CNTs always formed aggregates owing to very strong van der Waals interactions [7, 8].

Pulsed electric-current pressure sintering (PECPS), or spark plasma sintering (SPS), is a newly developed process, which can consolidate powder compact by applying an on-off dc electric pulse under uniaxial pressure [9]. During the sintering, a spark discharge at the narrow gaps between particles induces a high-temperature state locally. When a stacked powder exhibits a high electrical conductivity, the dc pulse passes through the powder compact, generating (1) spark plasma, (2) spark impact pressure, (3) Joule heat, and (4) an electric field among the particles. In General, mechanical properties of polycrystalline inorganic materials depend much on their microstructures or nanostructures; higher densities and smaller grain sizes bring the materials excellent properties, such as high bending strength and fracture toughness. PECPS or SPS processes have been reported to enhance the densification of ceramics or metal powders at relatively low sintering temperatures and short soaking times in comparison with those for conventional hot pressing.

In the present study, PECPS was utilized to fabricate dense CNF/Al_2O_3 composites in order to retain the CNFs in the matrix, *i.e.*, not to form other compounds by the solid-state reaction. Their mechanical properties such as bending strength σ_b, Vickers hardness H_v and fracture toughness K_{IC}, as a function of CNF content and electrical resistivity were measured and discussed in relation with their microstructures.

Experimental

Fabrication of CNF-dispersed Al_2O_3 composites

Carbon nanofiber (CNF) ''VGCF-H'' (~150 nm in diameter and 4~5 μm in length, ~99% purity, Showa Denko K.K., Tokyo, Japan) and a various kinds of α-Al_2O_3 powders namely, ''AES-23'' (average particle size (P_s) of ~1.1 μm, 99.9% purity) produced by the conventional Bayer method, and sol-gel derived high purity (>99.99%) ''AKP-20'' (P_s of ~0.5 μm), ''AKP-30'' (P_s of ~0.3 μm), and ''AKP-50'' (P_s of ~0.2 μm), which were supplied from Sumitomo Chemical Co., Ltd., Osaka, Japan, were used as starting materials. Zeta potentials of CNFs and 4 kinds of Al_2O_3 powders in the dilute aqueous suspensions (0.01wt%) were measured with a zeta potential analyzer (''Photal *Z*-1000'', Otsuka Electronics Co., Ltd., Osaka, Japan). Each sample was ultrasonicated for 15 min prior to measurement.

Before mixing CNFs with α-Al_2O_3 powders, the former CNFs were pre-dispersed into regent grade 2-propanol using an ultrasonic vibrating homogenizer with a power output of 300 W at frequency of 20 kHz (''US-300T'', Nihonseiki Ltd., Tokyo, Japan) for 15 min. After α-Al_2O_3 powder was added into the solution, mixed slurries with the compositions of CNF/Al_2O_3 = 0/100~10/90vol% were homogenized using the same ultrasonic vibrator for 15 min. Powder mixtures were prepared by drying the slurries with stirring at room temperature in air. The mixtures were uniaxially pressed into disks with a 16-mm diameter and a ~5 mm thick at 30 MPa. The compressed powder compact was put into a cylindrical mold (16 mm^{Φ}–40 mm^{Φ}–40 mm^{h}, high-density graphite carbon) that was used for a pulsed electric-current pressure sintering apparatus (''SPS-5104A'', Sumitomo Coal Mining Co., Ltd., Tokyo, Japan). Green densities of compressed mixtures were 2.20 for pure Al_2O_3 (AKP-30) and 2.02 $Mg{\cdot}m^{-3}$ for 5vol%CNF/95vol%Al_2O_3(AKP-30) powders; these values corresponded to 55.1% and 52.0% of their theoretical densities, 3.987 and 3.89 $Mg{\cdot}m^{-3}$, respectively, which were calculated using the theoretical densities of 3.987 for α-Al_2O_3 [10] and 2.0 $Mg{\cdot}m^{-3}$ for CNFs [11]. Using the PECPS apparatus, sintering was performed at 1200° to 1300°C for 5 min under an uniaxial pressure of 30 MPa in a vacuum (~10^{-2} Pa) with a heating rate of 100°C/min and a cooling rate of ~50°C/min, applying dc electric-current (on/off pulse interval = 12:2) the mold, plungers, and the sample. Heating temperature was measured at the center position about 5 mm far from the inside wall of carbon mold using a Pt–Rh thermocouple (JIS B-type: Pt/Rh30%–Pt/Rh6%, 0.5 mm^{Φ}).

Because dense monolithic α-Al_2O_3 ceramics, their bulk density being 3.96 $Mg{\cdot}m^{-3}$ i.e., 99.3% of theoretical density, were obtained at 1300 °C, as will be described later, CNF-dispersed Al_2O_3 composites were also sintered at the same temperature. To study the effect of CNFs addition to Al_2O_3 powder compact during sintering, shrinkage profiles of the powder compacts (monolithic and 5vol%CNF/Al_2O_3 composites) were taken in the same direction of applying pressure. Before and after sintering, SEM (FE-SEM, ''S-4300'', Hitachi, Co., Ltd., Tokyo, Japan) observation was conducted on the fracture surfaces of the powder and sintered compacts to investigate the dispersion of CNFs in the Al_2O_3 powder with various particle sizes.

Evaluation of microstructures and mechanical and electrical properties of sintered compacts

After cutting and lapping with a diamond saw and a diamond paste (nominal size 1~3 μm), respectively, bulk densities of the sintered materials were measured by Archimedes method. X-ray diffraction (XRD) analysis using Cu$K\alpha$1 radiation with a graphite monochromator was utilized for determination of their crystalline phases. After phase identification, testing samples for mechanical-property measurements were cut from the ceramics with a diamond saw and then polished the four sides to mirror surface with a diamond paste. Three-point bending strength σ_b was measured under the conditions of cross-head speed of 0.5 mm/min and an 8 mm span length. Vickers hardness H_v and fracture toughness K_{IC} were evaluated; measuring conditions for H_v were that an applying load of 19.6 N and a duration time of 15 s, and the indentation fracture method (IF) with Niihara's equation [12] were adopted to determine the K_{IC} values. Direct current (dc) electrical resistivity (ρ) of monolithic and composite materials were measured at room temperature by van der Pauw method [13] using the samples with four Ag-electrodes formed on their surfaces.

Results and discussion

Preliminary experiments revealed that the powder with P_s of ~0.3 μm (AKP-30) could be regarded as a representative of the α-Al_2O_3 powders used in this study; AKP-30 powder represented the characteristics of sintering process and sintered bodies.

Consolidation of monolithic Al_2O_3 powder with P_s of ~0.3 μm

The shrinkage of powder compact was in situ monitored during PECPS process. Figure 1(i) shows the displacement profile of *Z*-axis parallel to the pressing direction as a function of soaking time. The shrinkage curve was divided into two step-regions: (1) room temperature (R.T.)~900°C and (2) 900°–1300°C; in the former region a thermal expansion of green powder compact was observed and a rapid shrinkage of sample was recognized in the latter. Figure 2 shows SEM photographs of fracture surfaces for samples obtained at (a) 1200° and (b) 1250°C, indicated by arrows in Fig. 1(i); their average grain size (G_s) determined by an intercept method [14] were ~0.3 and ~0.6 μm, respectively. These samples having relative densities of (a) ~91.0% and (b) ~97.3% revealed that both temperatures were not enough to fabricate dense Al_2O_3 ceramics (≥99.0%). Dense monolithic Al_2O_3 ceramics with a high relative density of 99.3% could be obtained at 1300°C by PECPS, in addition as will be shown in the later figures, exhibiting homogeneous and well-developed microstructures consisting of G_s 4.4 μm (Table 1). From this result, the sintering temperature using PECPS was fixed at 1300 °C.

Dispersion of CNFs into α-Al_2O_3 powders with various particle sizes

Figure 3 displays an SEM photograph of weak agglomerated carbon nanofibers, CNFs (''VGCF-H''), used in this study after ultrasonicating in 2-propanol, showing straight fibers with a constant diameter (~150 nm) along the fiber length (~4–5 μm). Small semispherical tips are transition metal particles utilized as catalyst at a growth temperature of 1000–1300 °C during the production of CNFs by a vapor-grown carbon fiber (VGCF) method [2]. As CNFs were graphitized after VGCF process by heating near 3000 °C, amorphous carbon thin layer (~5 nm) was formed on the external surface of CNFs [2]. Dispersion of CNFs in the Al_2O_3 powders was confirmed by SEM observation on the fracture surface of the compressed powder compacts. Figure 4(a) indicates a strong agglomeration of CNFs

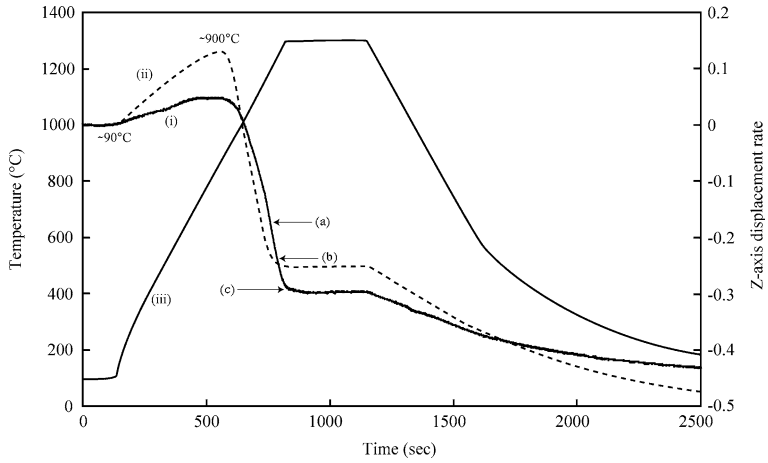

Fig. 1 Shrinkage profiles of (i) pure Al_2O_3 powder (AKP-30, P_s~0.3 μm) compact and (ii) a mixed powder compact with the composition of CNFs/Al_2O_3(AKP-30) = 5:95vol%, and (iii) a heating temperature as a function of soaking time; (**a**), (**b**) and (**c**) denote *Z*-axis displacements rates for pure Al_2O_3 powder compact at 1200 °C, 1250 °C and 1300 °C, respectively

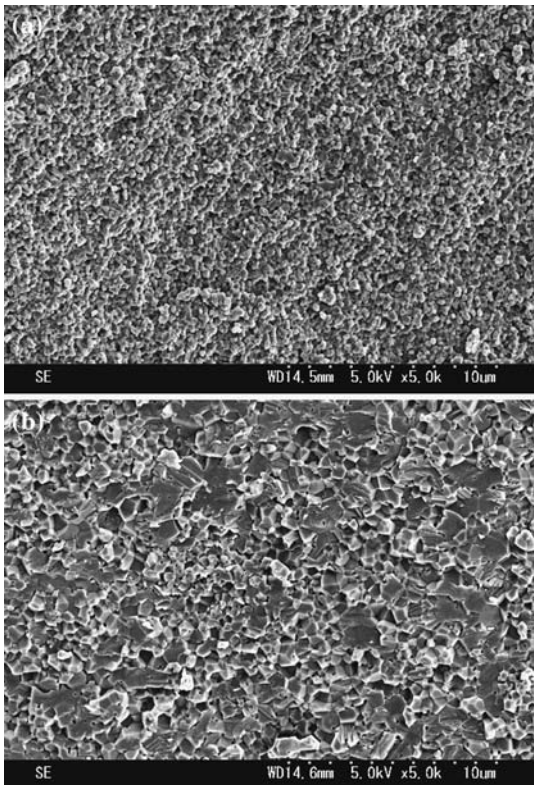

Fig. 2 SEM photographs for fracture surfaces of monolithic Al_2O_3 ceramics sintered for 5 min at (**a**) 1200 °C and (**b**) 1250 °C as indicated in Fig. 1

among large Al_2O_3 powders with P_s of ~1.1 μm, however, Fig. 4(b–d) reveal no agglomeration of CNFs in the powder compacts, in addition, (5vol%) fibers were dispersed well in the Al_2O_3 powders consisting of particles of which P_s are less than 0.5 μm.

To investigate the other factors affecting the dispersion of CNFs in the matrix, zeta potential (ζ) of the starting materials was measured. It was reported that the CNTs were negatively charged, and carbon black and CNTs

Table 1 Characteristics of monolithic Al_2O_3 and carbon-nanofiber(CNF)/Al_2O_3 composite materials fabricated by PECPS at 1300 °C and 30 MPa for 5 min in a vacuum

Contents of CNF (vol%)	Theoretical density ($Mg{\cdot}m^{-3}$)*	Bulk density ($Mg{\cdot}m^{-3}$)	Relative density (%)	Grain size of Al_2O_3 matrix
0 (pure Al_2O_3)	3.987	3.96	99.3	4.4
1	3.967	3.94	99.3	3.2
3	3.927	3.88	98.8	1.7
5	3.888	3.85	99.0	1.7
10	3.788	3.71	97.9	1.6

* calculated using theoretical densities of $D_x(Al_2O_3)$=3.987 $Mg{\cdot}m^{-3}$ [10] and D_x(CNF)=2.00 $Mg{\cdot}m^{-3}$ [2]

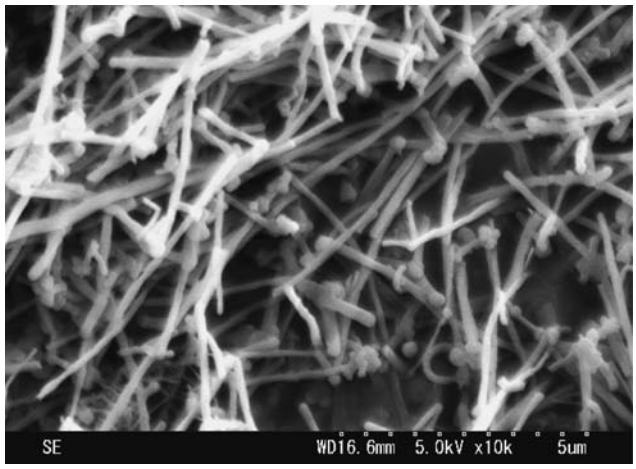

Fig. 3 An SEM photograph of carbon nanofibers (CNFs)

revealed a very similar shape to curve of ζ *vs*. pH plots [8]. Therefore, zeta potential ζ for the CNFs was thought to be a similar of the pristine CNTs: the ζ value of CNFs near pH~7 was –23 mV in contrast to –18 mV for CNTs [8]. On the other hand, the ζ for the Al_2O_3 powders with various P_s revealed almost constant values (+4.5 ~ –0.9 mV), which are consistent with the previous reported values (+20 ~ –10 mV at pH 6.5 ~ 7.5) for α-Al_2O_3 powder (P_s:0.03–0.1 μm in diameter [8]).

From these results, it might be concluded that the dispersion of CNFs depended much on the P_s of starting Al_2O_3 powders; good dispersion could be achieved in fine Al_2O_3 less than ~0.5 μm. This might be confirmed in the consolidated compacts sintered at 1300 °C for 5 min under 30 MPa by PECPS. Figure 5 shows SEM photographs for fracture surfaces of 3vol%CNF added composite materials fabricated from Al_2O_3 powders with P_s of (a) ~1.1 μm and (b) ~0.3 μm; agglomeration of CNFs was clearly recognized in the former sample and good dispersion was observed in the latter. These photographs also support the above-mentioned conclusions. Hereafter, only α-Al_2O_3 powder (AKP-30) with P_s of 0.3 μm was utilized in this study.

Microstructure of CNF/Al_2O_3 composite materials

Monolithic and composite materials with the compositions of CNF/Al_2O_3 = 0:100, 1:99, 3:97, 5:95, and 10:90vol% were fabricated by PECPS at 1300°C for 5 min under 30 MPa. A shrinkage profile for a 5vol%CNF dispersed Al_2O_3 powder compact was also shown in Fig. 1(ii). In comparison with that for monolithic Al_2O_3 powder compact as-mentioned in 3.1, a composite powder compact exhibited both a large expansion between R.T. and ~900 °C and a relative moderate shrinkage above ~900 °C up to 1300 °C; this might be due to a higher thermal

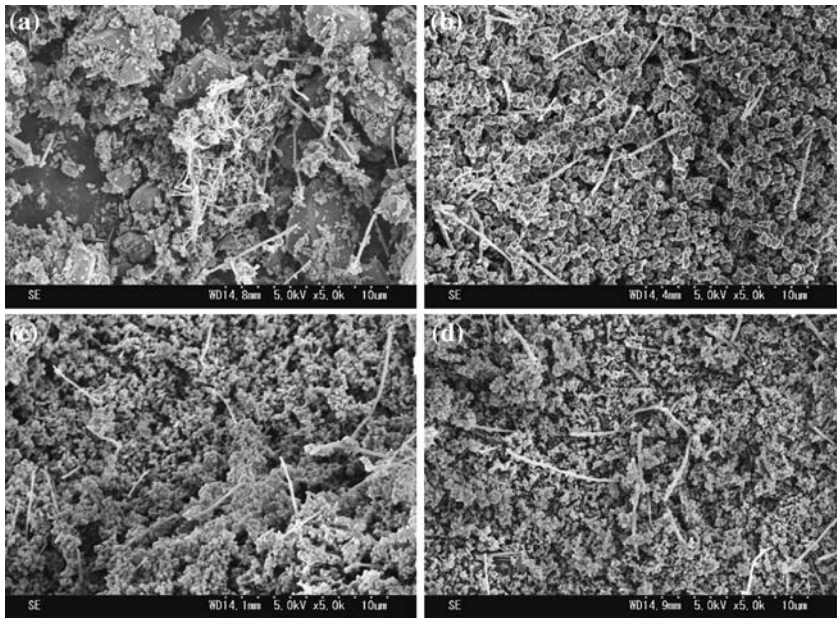

Fig. 4 SEM photographs for fracture surfaces of compressed powder compacts; 5vol%CNFs were dispersed into α-Al_2O_3 powders with the average particle size P_s of (**a**) ~1.1 μm, (**b**) ~0.5 μm, (**c**) ~0.3 μm, and (**d**) ~0.2 μm

expansion coefficient (~27×10^{-6}/K [15]) of graphite[1] normal to *c*-axis than that (~8.8×10^{-6} /K [15]) for polycrystalline Al_2O_3. As the relative density (52.1%) of the 5vol% CNF added powder compact was a little lower than that (55.1%) of monolithic powder compact, and further the relative densities of sintered materials were almost the same (99.3% for monolithic and 99.0% for composite, as indicated in Table 1), the *Z*-axis displacement rate (–0.45) of the composite at room temperature was a little larger than that (–0.43) for monolithic sample as shown in Fig. 1(i) and (ii). Figure 6 shows XRD patterns of pulverized samples from (a) monolithic Al_2O_3, (b) 3vol%CNF/Al_2O_3, (c) 5vol%CNF/Al_2O_3 and (d) 10vol% CNF/Al_2O_3 composite materials sintered at 1300°C. In the samples with 0vol% (monolithic) and 1vol%CNF addition only α-Al_2O_3 (corundum) peaks were observed, however, more than 3vol%, graphite *(002)* different peak was detected. This was explained in terms of the small fraction of CNFs in the composites; only the most intensive peak (*002*) at $2\theta \sim 25.94°$ (Cu$K\alpha$) [17] could be noticed. Furthermore, any other peaks were not recognized. This could suggest either no solid-state reaction between CNFs and Al_2O_3 during PECPS or too small amounts of compounds formed between amorphous carbon thin layer on the surface of CNFs and fine α-Al_2O_3 powder. Based on the former, the XRD results supported the occurrence of CNFs in the composites, as will be proved in the later by direct SEM observation. And in the latter case, strong cohesion force between CNFs and Al_2O_3 would be present.

[1] Thermal expansion coefficient α of carbon nanofiber has not been reported, irrespective of many reports of carbon nanotubes [1, 16].

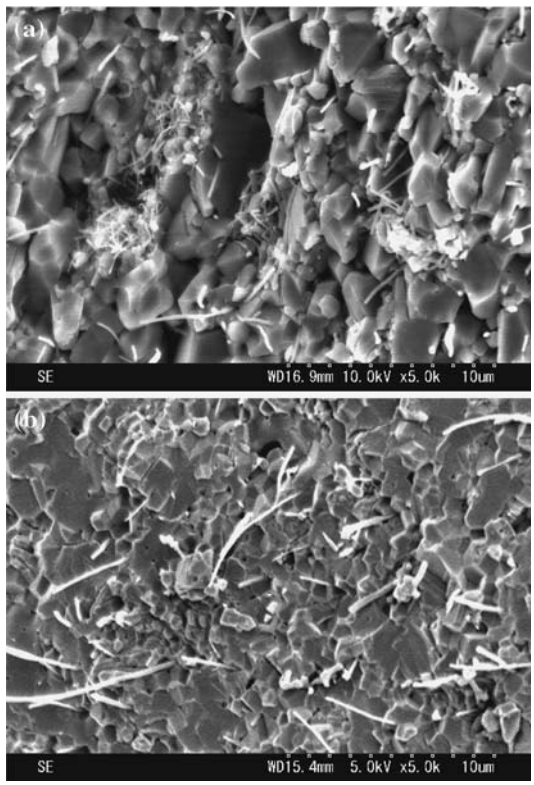

Fig. 5 SEM photographs for fracture surfaces of sintered composite materials fabricated from (**a**) α-Al_2O_3 (P_s ~1.1 μm) and (**b**) α-Al_2O_3 (P_s ~0.3 μm); 3vol%CNFs were dispersed to both materials and sintered at 1300 °C for 5 min under 30 MPa in a vacuum

Figure 7 exhibits SEM photographs for fracture surfaces of (a) monolithic Al_2O_3, (b) 5vol%CNF/Al_2O_3, and (c) 10vol%CNF/Al_2O_3 composite materials. Dense homogeneous microstructure consisting of large Al_2O_3 grains of

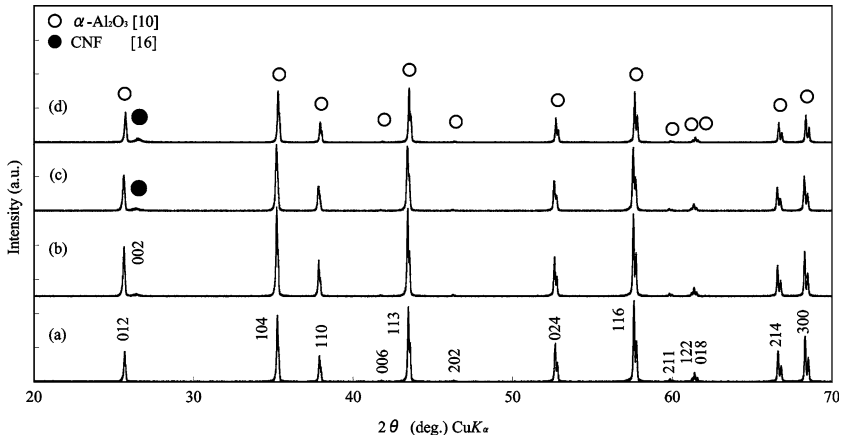

Fig. 6 XRD patterns of pulverized samples from (**a**) monolithic Al_2O_3, (**b**) 3vol%CNF/Al_2O_3, (**c**) 5vol%CNF/Al_2O_3 and (**d**) 10vol%CNF/Al_2O_3 composite materials: the same? α-Al_2O_3 powder (P_s~0.3 μm) was used

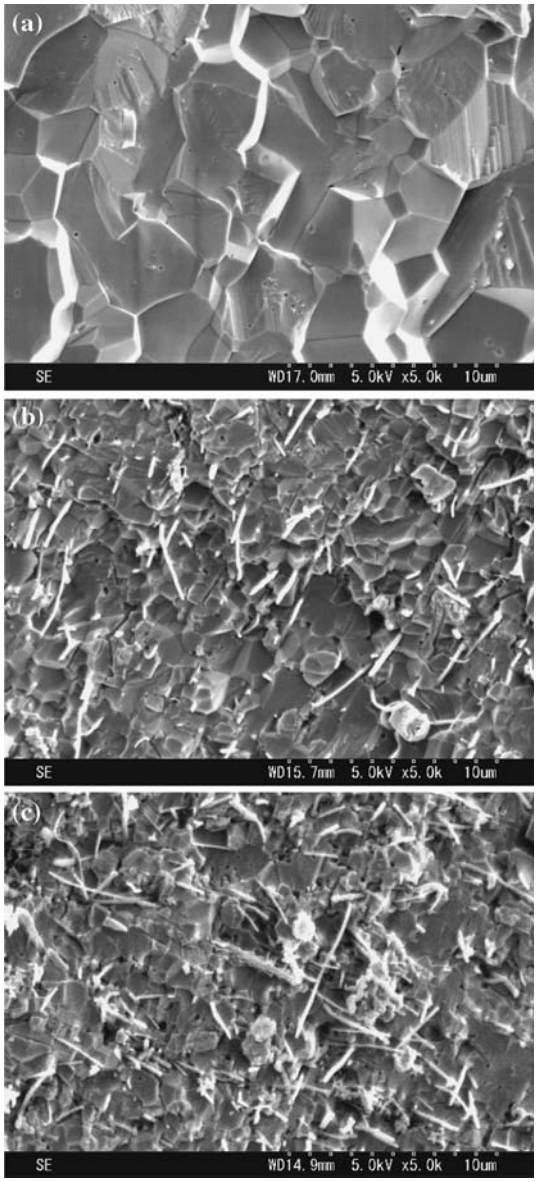

Fig. 7 SEM photographs for fracture surfaces of (**a**) monolithic Al_2O_3, (**b**) 5vol%CNF/Al_2O_3, and (**c**) 10vol%CNF/Al_2O_3 composite materials

4.4 μm was observed in the monolithic Al_2O_3 ceramics (Fig. 7(a)), indicating that the sintering conditions of 1300°C/5 min/30 MPa was suitable to fabricate dense Al_2O_3 ceramic materials in which Al_2O_3 grains had grown to ~4.4 μm under this condition. Long carbon nanofibers aligned in the Al_2O_3 matrix were recognized in the fracture surfaces of the samples with 5 and 10vol% CNF additions (Fig. 7(b) and (c)), suggesting weak cohesion bonding between CNFs and Al_2O_3 matrix, if strong bonding was formed CNFs could not be pulled-out as easily as this. CNFs bridging grain boundaries showed that the fibers were retained in the composites without any other particles or segregations. Table 1 shows characteristics of monolithic and composite materials sintered at 1300 °C for 5 min under 30 MPa. Bulk and relative densities decreased gradually with increasing CNF content from 3.96 (99.3) to 3.71 (97.9%) $Mg{\cdot}m^{-3}$, indicating that CNF addition suppressed the sinterability of Al_2O_3 powder, however, it should be noted that a high relative density of 99.0% was attained up to 5vol%CNF addition. Average grain size (G_s) of Al_2O_3 matrix also decreased from 4.4 to 1.6 μm with increasing amount of CNF, revealing that CNF had much effect on grain growth during PECPS as an inhibitor; a 5vol%CNF/Al_2O_3 composite had G_s less than 1/2 of monolithic material.

Mechanical and electrical properties of CNF/Al_2O_3 composite materials

From an investigation viewpoint of CNFs addition-effect on Al_2O_3 ceramics, as has been much expected previously but not succeeded yet, mechanical properties of composite materials were evaluated. Figure 8 displays (a) three-point bending strength σ_b, (b) Vickers hardness H_v, and (c) fracture toughness K_{IC} as a function of CNF volume content. Data present the average values obtained from five test specimens. Bending strength σ_b increased monotonously from ~645 (monolithic) to ~800 MPa at 5vol%CNF addition and then decreased gradually to ~525 MPa

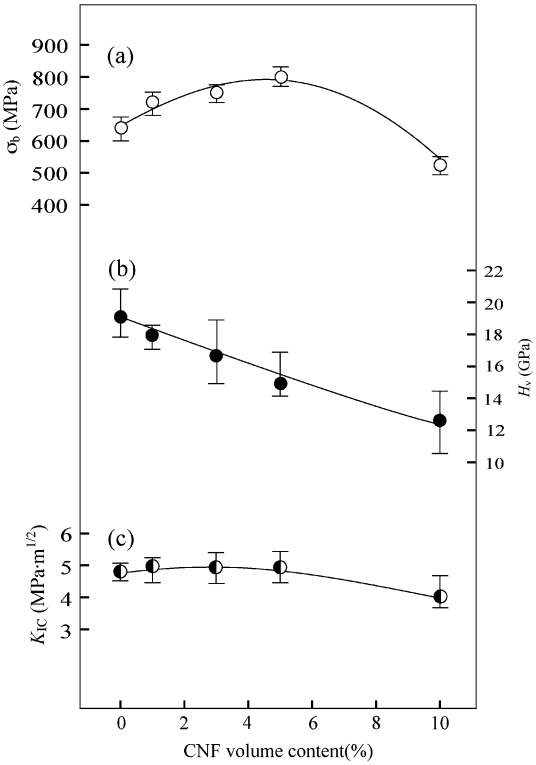

Fig. 8 Mechanical properties of CNF/Al_2O_3 composite materials: (**a**) three-point bending strength σ_b, (**b**) Vickers hardness H_v, and (**c**) fracture toughness K_{IC} of CNF/Al_2O_3 composite materials as a function of CNF volume content

(10vol%CNF/Al_2O_3 composite). Concerning about flexure strength, or bending strength of inorganic polycrystalline materials, there is a linear relationship between strength s and the inverse square root of grain size ($G_s^{-1/2}$); the smaller G_s the higher s if the densities of materials are not changed [18]. Therefore, the former increment might be due to the decrease in G_s of alumina matrix with the almost same density (Table 1) and the latter reduction could be explained in terms of the poor cohesion force between CNFs and the Al_2O_3 as suggested by Laurent et al. [6].

On the contrary, hardness H_v decreased monotonously with increasing CNF content as shown in Fig. 8(b). Although no apparent G_s dependence of H_v for Al_2O_3 ceramics with 90–99.9% relative densities was reported by Alpert et al. [19], more recent data of Krell' and Blank [20] on Al_2O_3 with G_s extending from ~4 down to ~0.4 μm generally agrees with the trends and absolute values of other data reported, clearly showing a substantial increase in H_v as G_s decreases. If it could be based on both the latter report and the rule-of-mixtures as indicated in Eq. (1) [21],

$$H_v(\text{composite}) = (1 - v_f) \times H_v(\text{matrix}) + v_f \times H_v(\text{second phase}) \quad (1)$$

where, v_f is the volume fraction of second phase or dispersed particles, H_v(matrix) the intrinsic hardness of matrix, and H_v(second phase) the hardness of second phase. Here, it must be noted that Eq. (1) is an approximation; it is often a useful tool, but it may not be feasible to adequately incorporate effects of second phase. Increase in H_v brought by the smaller grain size of matrix might be much more reduced by low H_v(second phase), i.e., H_v(CNF).

Until now the tensile modulus (E_t) of CNFs (VGCF) was estimated to be 100–300 GPa [2], however, its intrinsic hardness has not been cleared. On the other hand, it was reported that in inorganic materials H_v was proportional to E_t, i.e., $H_v \sim 0.05\ E_t$ [22]. The value of H_v(CNF) calculated from this relation was ~15 GPa; however, this value dose not agree with a negative value estimated from the data shown in Fig. 8(b) and Eq. (1).

An et al. [4] studied the tribological properties of Al_2O_3–CNT composites fabricated by hot pressing the mixed powders synthesized in the catalytic decomposition of acetylene over alumina powders impregnated with iron catalysis; they described that a maximum microhardness (19.6 GPa) was observed near 4wt% (7.67vol%) of CNT content and further addition of CNTs lowered the microhardness significantly due to both the difficulty in dispersing CNTs homogeneously in the composites and the problem of the poor cohesion force between CNTs and the matrix. Recently, Vickers hardness H_v of CNTs/Al_2O_3 composites fabricated via (i) molecular level mixing process [23], (ii) sol–gel process [24], and (iii) homogeneously CNTs dispersion to fine alumina powders [25] have been investigated. The values obtained for the composites prepared by the former two processes are reported to be increased up to 0.5 or 3.0 vol% CNTs addition, respectively, due to an enhanced load sharing of CNTs distributed within the Al_2O_3 grains and the interfacial strength between CNTs and matrix. However, the latter composite gave a reduced H_v value. This difference could be explained as follows; due to the agglomeration of CNTs added more than 0.5 or 3.0 vol%, respectively, CNTs of which are located at the Al_2O_3 grain-boundaries, H_v values of the composites are decreased. However, these phenomena were not observed in the present study, irrespective of homogeneous dispersion of CNFs in the matrix; this might be due to large and thick carbon nanofibers (CNFs) compared with CNTs.

As shown in Fig. 8(c), a little increase was recognized in K_{IC} from 4.8 to 5.0 MPa m$^{1/2}$ at 3~5vol%CNT addition. Ning et al. [26] fabricated CNT/SiO_2 composites using MWCTs and 3.1 μm SiO_2 glass powders ultrasonicated, and investigated the effect of CNTs addition on the mechanical properties. They reported that K_{IC} increased from ~1.0 to ~2.0 MPa m$^{1/2}$ with an addition of 5vol%CNT, and then it was lowered to ~1.3 MPa m$^{1/2}$ by

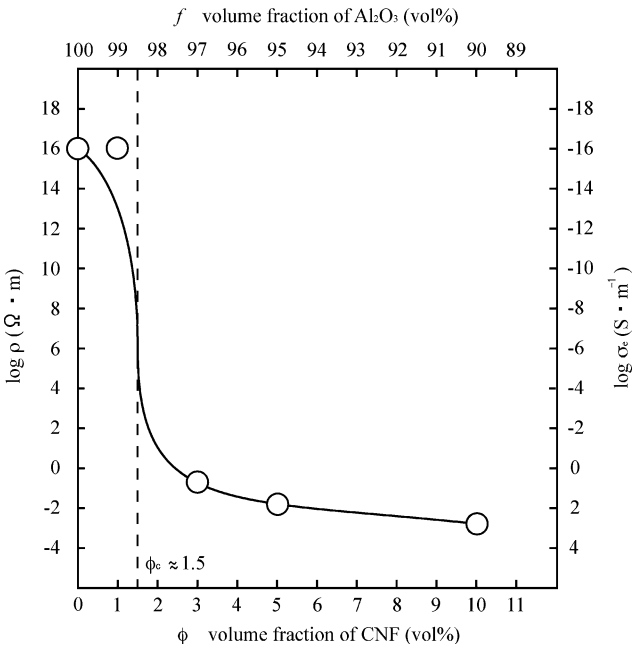

Fig. 9 Electrical resistivity ρ (conductivity σ_e) of CNF/Al_2O_3 composites as a function of CNF volume fraction ϕ (Al_2O_3 volume fraction $f = 1–\phi$); ϕ_c ($f_c = 1–\phi_c$) is the critical percolation volume of ~0.015 (~0.985) and t is the exponent ~2.98 for the percolation equation

further addition of 10vol%CNT. This behavior was also observed for the bending strength of the same CNT/SiO_2 composites. As far as concern of CNT/Al_2O_3 composites, Siegel et al. [5] reported that the K_{IC} of 10vol% MWNT addition to nanophase alumina powder in which MWNT was dispersed with an ultrasonic prove, increased by ~24% from ~3.4 to ~4.2 MPa $m^{1/2}$, and explained that by the microstructure observation on the fracture surfaces, damage delocalization had been occurred as a result of homogeneously dispersed nanotubes in the matrix. Laurent et al. [6] fabricated the CNT–Fe–Al_2O_3 nanocomposites by hot pressing and measured their fracture strength σ_f and fracture toughness K_{IC}. They described that σ_f values (~553 MPa) of most nanocomosites thus fabricated were only marginally higher than that (~330 MPa) of Al_2O_3, but lower than those (~600 MPa) of corresponding Fe-Al_2O_3 composites and K_{IC} values (3~5 MPa·$m^{1/2}$) were generally markedly lower than those (~7.5 MPa·$m^{1/2}$) of CNT-free Fe–Al_2O_3 composites. By comparing these data with present experimental results, the former two results, *i.e.*, simultaneous increase of σ_b and K_{IC} in the present study, should be noted because as above-mentioned, previous researches reported that CNTs addition to Al_2O_3 did not necessarily enhance their mechanical properties.

Direct current (dc) electrical resistivity (ρ_m) of CNF/Al_2O_3 composite materials measured at room temperature were $>10^{15}$ (0 and 1vol%CNFs), $\sim 2.2 \times 10^{-1}$ (3vol%), $\sim 2.1 \times 10^{-2}$ (5vol%), and $\sim 1.7 \times 10^{-3}$ Ωm (10vol%), respectively. Figure 9 illustrates the electrical resistivity ρ_m (electrical conductivity, $\sigma_e = 1/\rho_m$) of composite materials as a function of CNF volume content ϕ (Al_2O_3 volume content, $f = 1–\phi$). This drastic change in ρ_m (σ_e) could be explained by percolation theory [27]: $\rho_m = \rho(Al_2O_3) \times 1- \phi/\phi_c)^t$ [or $\sigma_e = \rho(CNF)^{-1} \times 1\text{-}f/f_c)^t$] using ρ(CNF) of 1×10^{-6} Ωm [2], $\rho(Al_2O_3)$ of $\sim 10^{16}$ Ωm [28], critical percolation volume fraction ϕ_c of ~0.015 ($f_c = 1–\phi_c = 0.0985$), and an exponent for the percolation t of ~2.98. The latter two parameters were determined from the present experimental data. Up to now, alumina has not been processed by an electric discharge machining [29], which demands a low electrical resistivity bellow $\sim 1 \times 10^0$ Ωm for materials and by which processing hard bulk materials with precise and complicated shapes can be manufactured in a short time. However, it has been cleared that 3–5vol%CNF added alumina reveals the machinability of electric discharge process despite of deterioration of the mechanical properties. On the other hand, in the present composite materials, there is little difference in ρ_{par} measured parallel to and ρ_{per} perpendicular to the PECPS pressing direction; for example, in the 5vol%CNF/Al_2O_3 composites, the former and the latter were 2.14×10^{-2} and 2.10×10^{-2} Ωm, respectively. This data also supports the homogeneous dispersion of CNFs in the matrix.

Conclusions

Dense carbon-nanofiber(CNF)/Al_2O_3 composite materials with addition up to 10 vol%CNF were fabricated by pulsed electric-current pressure sintering at 1300 °C for 5 min under 30 MPa in a vacuum. By comparing with monolithic Al_2O_3 ceramics, their microstructures and mechanical properties were evaluated. A small amount of CNFs homogeneously dispersed into fine Al_2O_3 powders with particle size less than ~0.5 μm suppressed the grain growth of Al_2O_3 during PECPS from 4.4 (monolithic) to 1.6 μm (5vol%CNF). Their bending strength σ_b and fracture toughness K_{IC} revealed the maximum values, ~800 MPa and ~5 MPa·$m^{1/2}$, respectively, near 5vol% addition. On the other hand, Vickers hardness H_v decreased monotonously. These experimental results might be interrupted in terms of relatively homogeneous dispersion of CNFs and weak cohesion bonding between CNFs and Al_2O_3 grains. The latter problem is still left to must be solved in future.

Acknowledgements This work was supported by a grant to Research Centre for Advanced Science and Technology at Doshisha University from the Ministry of Education, Culture, Sports, Science and Technology, Japan.

References

1. Iijima S (1991) Nature 354:56
2. Endo M, Kim YA, Hayashi T, Nishimura K, Matushita T, Miyashita K, Dresselhaus MS (2001) Carbon 39:1287
3. Hammel E, Tang X, Trampert M, Schmitt T, Mauthner K, Eder A, Pötschke P (2004) Carbon 42:1153
4. An J-W, You D-H, Lim D-S (2003) Wear 255:677
5. Siegel RW, Chang SK, Ash BJ, Stone J, Ajayan PM, Doremus RW, Schadler LS (2001) Scripta Mater 44:2061
6. Laurent Ch, Peigney A, Dumortier O, Rousset A (1998) J Euro Ceram Soc 18:2005
7. Jiang L, Gao L, Sun J (2003) J Colloid Interface Sci 260:89
8. Sun J, Gao L (2003) Carbon. 41:1063
9. Tokita M (1993) J Soc Powder Tech Jpn 30:790
10. Powder Diffraction File, Card No. 46–1212, International Centre for Diffraction Data, Newtown Square, PA, 2001
11. CNF Catalogue from the supplier (Showa Denko K.K.) 2001. (http://www.sdk.co.jp/contents/product/index.htm)
12. Hiihara K, Morena R, Hasselman DPH (1982) J Mater Sci Lett 1:13
13. van der Pauw LJ (1958) Philips Rep 13:1
14. Mendelson MI (1969) J Am Ceram Soc 52:443
15. Kingery WD, Bowen HK, Uhlmann DR (1976) In: Introduction to ceramics, 2nd ed. John Wiley & Sons, NY, p 595
16. Thostenson ET, Ren Z, Chou T-W (2001) Composites Sci Tech 61:1899
17. Zhu YQ, Zhang HG, Zhang JH, Liang J, Gao ZD, Wei BQ, Wu DH, Hui MJ (1994) J Mater Sci Lett 13:1104
18. Rice RW (2003) In: Mechanical properties of ceramics and composites – grain and particle effects. Marcel Dekker, Inc. NY, p 127
19. Alpert CP, Chan HM, Bennison SJ, Lawn BR (1988) J Am Ceram Soc 71:C371
20. Krell A, Blank (1993) J Am Ceram Soc 78:1118
21. Rice RW (2003) In: Mechanical properties of ceramics and composites – grain and particle effects. Marcel Dekker, Inc. New York, Basel, pp 601
22. Tanaka K, Koguchi K, Mura T (1989) Int J Eng Sci 27:11
23. Cha SI, Kim KT, Lee KH, Mo CB, Hong SH (2005) Scripta Mater 53:793
24. Mo CB, Cha SI, Kim KT, Lee KH, Hong SH (2005) Mater Sci & Eng A395:124
25. Sun J, Iwasa M, Nakayama T, Niihara K (2004) J Ceram Soc Jpn 112:S403
26. Ning J, Zhang J, Pan Y, Guo J (2003) Mater Sci & Eng A357:392
27. McLachlan DS, Blaszkiewicz M, Newnham RE (1990) J Am Ceram Soc 73:2187
28. Shackelford JF, Alexander W (2001) In: Material science and engineering handbook, 3rd ed. CRC Press, NY, p 959
29. Petrofes NF, Gadalla AM (1988) Am Ceram Bull 67:1048